

Signature splitting and signature inversion of rotational bands in odd-odd nuclei in rare-earth region

Manal Mahmoud SIRAG

Department of Physics, Girls College, Ain Shams University
Cairo-EGYPT
e-mail: dm_sirag@yahoo.com

Received 10.04.2009

Abstract

Anomalous signature splitting and signature inversion for the configuration $\pi h_{11/2} \otimes \nu i_{13/2}$ in rotational bands of odd-odd nuclei have been studied using the energy staggering index $S(I)$ as a function of spin I . The unfavored signature index was found lying lower than the favored one. A systematic look at the features of this signature inversion in a series of nine lighter rare earth nuclei in the region around $A \sim 160$ ($Z = 65 - 75$, $N = 89 - 101$) are presented. The analysis reveals an anomalous signature splitting for this configuration. The magnitude of signature splitting at low spins decreases as the proton number increases. The large signature splitting between the favored and the unfavored bands are observed in ^{156}Tb . The signature inversion point remains fairly constant for nuclei with the same value of $N - Z$ and decreases when $N - Z$ increases.

Key Words: Signature splitting, signature inversion, staggering.

1. Introduction

Spectroscopic information on high-spin states of odd-odd nuclei near $A = 150 - 170$ provide a suitable insight to studying the interplay between the single particle and collective motion, and for probing the residual neutron-proton interaction. As is well known, the structure of odd-odd nuclei is the most complex encountered experimentally, and thus results on such nuclei have been published at a very slow rate during past decades. Most comprehensive studies combine high-resolution results from neutron capture gamma-ray spectroscopy and from direct transfer reactions [1, 2]. Therefore, only low-spin states of neutron rich nuclei adjacent to stable odd-even isotopes can be investigated in this way. With the arrival of high-energy heavy-ion beams and improved γ -ray detection techniques using the multidetector- array, it has become possible to study excited states in collectively rotating nuclei up to high spins [3–16]. Several striking features such as identical bands [17–

20], band crossing [21, 22] and anomalous signature splitting and signature inversion bands on the $\pi h_{11/2} \otimes \nu i_{13/2}$ Nilsson configuration [10, 11, 23–27] were investigated. Signature splitting refers to the energy difference between the two signature sequences of one rotational bands.

The signature dependence in odd-odd nuclei can be considered by cranked shell model as follows: if the last proton and the neutron are sitting in unique-parity high-j orbitals, four rotational sequences connected by electric quadrupole transitions could be built. From the additivity rule, the sequences can be classified into the following categories, namely,

- (a) $I = (j_p + \text{even}) + (j_n + \text{even})$
- (b) $I = (j_p + \text{even}) + (j_n + \text{odd})$
- (c) $I = (j_p + \text{odd}) + (j_n + \text{even})$
- (d) $I = (j_p + \text{odd}) + (j_n + \text{odd}).$

The total angular momenta of the proton and the neutron are denoted by j_p and j_n . The sequence (a) is favored, the sequences (b) and (c) are unfavored and the last sequence (d) is very unfavored.

A particular exotic feature in odd-odd nuclei is that the Routhians corresponds to the two signatures $\alpha = 0, \alpha = 1$ of the band are crossing each other at a rotational frequency characteristic of the nucleus. This behavior was not expected, since it is not observed in the odd-A nuclei. The values corresponding to the unfavored signature states lie relatively lower in energy than the favored signature ones at low spins (anomalous signature splitting). The inverse situation is observed at higher spin. At some critical frequency a signature crossing does occur. An anomalous signature splitting is not observed in odd-A nuclei, especially before band crossing.

There are several theoretical attempts [23, 24, 28–35] to interpret signature inversion in the $\pi h_{11/2} \otimes \nu i_{13/2}$ bands of odd-odd rare-earth nuclei. The signature inversion analyzed in the framework of the cranked shell model by introducing a positive triaxial deformation of the rotating nucleus when the proton Fermi surface lies in the vicinity of the $K = 5/2$ or $K = 7/2$ [23, 24, 30]; also the calculations based on a particle-rotor model [31–33] suggest that an axially symmetric shape can well explain the observed signature inversion. Another approach within the framework of an axially symmetric rotor plus two particles model [34, 35] suggest that the signature inversion is a result of Coriolis mixing between the large number of bands arising from coupling of the $i_{13/2}$ neutron and the $h_{11/2}$ proton orbitals. Other explanations have been attempted using the angular momentum projection approach [28, 29] which suggests two possible mechanisms for the signature inversion. One involves a self- inversion and the other involves a band crossing between two bands which have mutually opposite signature dependence. Also the signature inversion has been studied through interacting boson-fermion model [36]. In spite of these efforts, the essential mechanism for the signature inversion is still an open question.

In the present paper, we present analysis of signature splitting and signature inversion of yrast bands in $^{154,156}\text{Tb}$, ^{160}Ho , $^{162,166}\text{Tm}$, $^{166,168}\text{Lu}$, ^{174}Ta and ^{176}Re odd-odd nuclei, and discuss the mechanism of the behavior of dynamical moment of inertia.

2. Outline of the theory

The signature dependence of a rotational band is related to the K quantum number of associated single-particle states, and the deformation of the nucleus. In some bands of odd-odd nuclei, the energy signature

splitting is small compared with that of its neighboring odd-mass nuclei. In order to magnify this small energy signature splitting, on energy staggering index $S(I)$ defined as

$$S(I) = [E(I) - E(I-1)] - \{[E(I+1) - E(I)] + [E(I-1) - E(I-2)]\}/2 \quad (1)$$

is plotted as a function of spin I or rotational frequency $\hbar\omega$. Here $E(I)$ is the excitation energy of state I . We see that $S(I)$ is directly proportional to the energy difference $\delta(E)$ of the two signatures

$$\delta(E) = E(I) - [E(I+1) - E(I-1)]/2 \quad (2)$$

but magnified by a factor of two.

The band is split or classified into two bands favored and unfavored.

An illustration of bands and their crossings can be carried out in terms of dynamical moment of inertia $J^{(2)}$. An odd-odd deformed nucleus can generate angular momentum by rotation in which all the nucleons rotate collectively about an axis perpendicular to the symmetry axis and by alignment of the angular momenta of individual nucleus with rotation axis. The total angular momentum of a rotating deformed nucleus I , can be written as

$$\hat{I} = \hat{R} + \hat{J}, \quad (3)$$

where \hat{R} is the angular momentum generated by the rotation of the core, and \hat{J} is the sum of the intrinsic angular momenta of the unpaired valence nucleons, the extra proton and neutron.

If we chose Z-axis as the symmetry axis, then as \hat{R} is perpendicular to Z-axis, the projection of \hat{I} and \hat{J} onto the Z- axis is the same and is denoted by K . One can write

$$\hat{J} = \hat{j}_p + \hat{j}_n, K = \Omega_p + \Omega_n \quad (4)$$

Classically, the kinetic energy of a rotating rigid body is giving by

$$E_{rot} = \theta\omega^2/2, \quad (5)$$

where θ is the moment of inertia of the system and

$$\omega = \frac{I}{\theta} \quad (6)$$

is the angular rotational frequency.

Combining equations (5) and (6) and transforming from classical system to a quantum system leads to a sequence of states with energies

$$E(I) = \frac{\hbar^2}{2\theta} I(I+1). \quad (7)$$

Here, θ is the static moment of inertia (written as $J^{(0)}$). The rotational frequency is not directly measurable but it is related to the observed angular momentum I and the excitation energy $E(I)$ of the state.

The classical frequencies ω defines a quantum energy $\hbar\omega$:

$$\hbar\omega = \frac{dE(I)}{dI_x}, \quad (8)$$

where

$$I_x = [I(I+1) - K^2]^{1/2} \quad (9)$$

is the projection of the total angular momentum onto the rotational axis x. The nucleus, however, is not a rigid body, i.e. $J^{(0)}$ is not constant. As the nucleus rotates it is found that the moment of inertia changes as a function of spin. Rotational energy spectra can hence be discussed in terms of a spin dependent moment of inertia $J^{(1)}$ which is related to the first-order derivative of the excitation energy with respect to the aligned angular momentum I_x :

$$J^{(1)} = I_x \left(\frac{dE}{dI_x} \right)^{-1} \hbar^2 = \hbar \frac{I_x}{\omega} \quad (10)$$

The kinematic moment of inertia $J^{(1)}$ can be related to the transition energy E_γ as

$$\frac{2J^{(1)}}{\hbar^2} = \frac{4I-2}{E_\gamma}; E_\gamma = E(I) - E(I-2) \quad (11)$$

The second-order derivative of the excitation energy with respect to the aligned angular momentum I_x is the dynamic moment of inertia

$$J^{(2)} = \frac{d^2E}{dI_x^2} \hbar^2 = \hbar \frac{dI_x}{d\omega}. \quad (12)$$

The dynamic moment of inertia $J^{(2)}$ can be related to the difference in transition energy of consecutive γ -rays as

$$\begin{aligned} \Delta E_\gamma &= \frac{\partial E_\gamma}{\partial I} dI + \frac{\partial E_\gamma}{\partial J} dJ \\ &= \frac{2\hbar^2}{J} dI - \frac{\hbar^2}{J^2} (2I-1) dJ. \end{aligned} \quad (13)$$

Thus

$$\begin{aligned} \frac{\Delta E_\gamma}{\Delta I} &= \frac{2\hbar^2}{J} - \frac{1}{\theta} E_\gamma \frac{dJ}{dI} \\ &= \frac{2\hbar^2}{J} - E_\gamma \frac{d(\ln J)}{dI}. \end{aligned} \quad (14)$$

For transition $\Delta I = 2$, one obtains

$$\Delta E_\gamma = \frac{4\hbar^2}{J} - 2E_\gamma \frac{d(\ln J)}{dI}. \quad (15)$$

If the moment of inertia does not change very rapidly with I , we obtain

$$\Delta E_\gamma = \frac{4\hbar^2}{J^{(2)}}, \text{ or } J^{(2)} = \frac{4\hbar^2}{\Delta E_\gamma}, \quad (16)$$

with

$$\Delta E_\gamma = E_\gamma(I+2) - E_\gamma(I). \quad (17)$$

Thus, if the dynamical moments of inertia are constant, the transition energy difference would be the same for all values of spin.

The two moments of inertia can be related as follows:

$$\begin{aligned}
 J^{(2)} &= \frac{dI_x}{d\omega} \\
 &= \frac{d}{d\omega} (\omega J^{(1)}) \\
 &= J^{(1)} + \omega \frac{dJ^{(1)}}{d\omega}.
 \end{aligned} \tag{18}$$

In the limit of rigid rotation

$$J^{(2)} \approx J^{(1)}. \tag{19}$$

3. Calculations and systematics of the signature inversion

Rotational structures in nuclei can be characterized by the signature quantum number α which defines the admissible spin sequence for a band through the relation $I = \alpha + 2n$ ($n = 0, 1, \dots$).

This is a consequence of the well-known D2-symmetry of deformed intrinsic shapes reflected through the appearance of two signature partner bands with $\alpha = 0$ or 1 in even-mass nuclei. In a plot of the level energies $E(I)$ versus spin I usually each of the two signature branches forms regular $I(I + 1)$ sequence. One branch is favored by a lower change in energy, whereas the other one is separated by the so-called signature splitting. Usually, one expects that such a signature splitting would grow with spin I due to increase in Coriolis force. Quantitatively this splitting effect can be seen when plotting the energy differences $[E(I) - E(I - 1)]/2I$ as a function of I and appears as a typical staggering curve. However, one observes in several cases that the signature splitting decreases with spin and even changes its sign, i.e. the energetically favored and unfavored signature branches cross each other and interchange their roles. This phenomenon is known as signature inversion.

For the $h_{11/2}$ yrast bands in odd-Z and $i_{13/2}$ yrast bands in odd-N rare- earth nuclei, the favored signature partner lies lower in energy than the unfavored signature partner. On the other hand, for the $\pi h_{11/2} \otimes \nu i_{13/2}$ yrast bands in the neighboring odd-odd nuclei at rotational frequencies below ~ 0.2 MeV, the Routhian of the favored signature is found to lie higher in energy as compared to that of the unfavored signature. This is referred to as the anomalous signature splitting. As the rotational frequency is increased the two Routhians cross at a certain critical frequency above which signature inversion occurs.

We investigated the $\pi h_{11/2} \otimes \nu i_{13/2}$ bands in nine odd-odd nuclei up to high spins and found interesting anomalous signature splitting for this configuration. The energy difference $E(I) - E(I - 1)$ versus spin I are plotted in Figures 1–2 for these nine selected nuclei. The data source is reference [37] and the calculated values are listed in Tables 1–9. In Figures 1–2 the open circles represent the $\Delta I = 2$ transition sequence with favored signature $\alpha = 0$ and the filled circles for the unfavored one $\alpha = 1$.

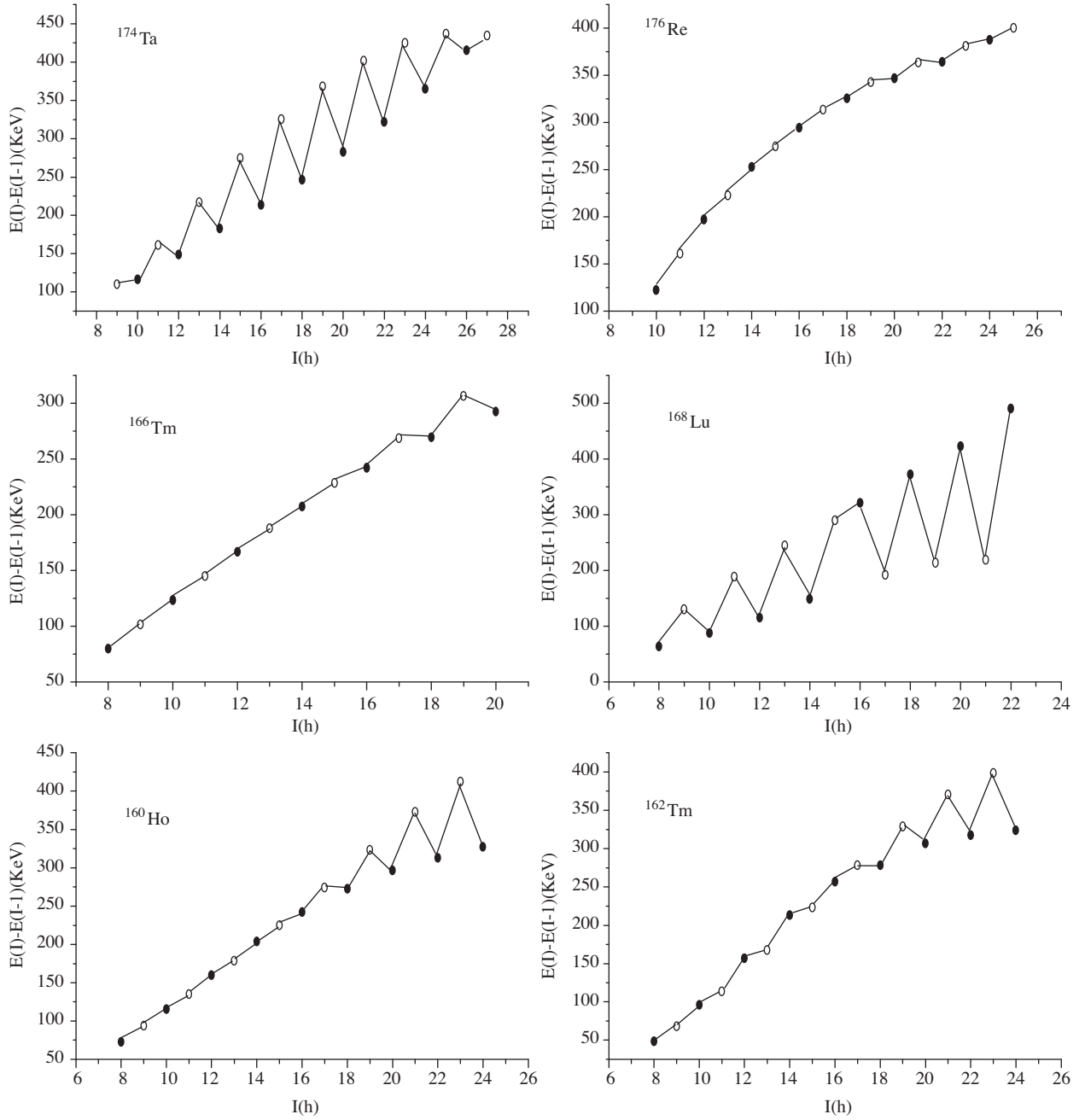


Figure 1. Variation of the energy difference between two consecutive levels $E(I) - E(I-1)$ of the $\pi h_{11/2} \otimes \nu i_{13/2}$ band as a function of spin I , for the odd-odd isotones $N = 93, 97$ and 101 . The open circles represent the $\Delta I = 2$ transition sequence with favored signature $\alpha = 0$, the filled circles for the unfavored one $\alpha = 1$.

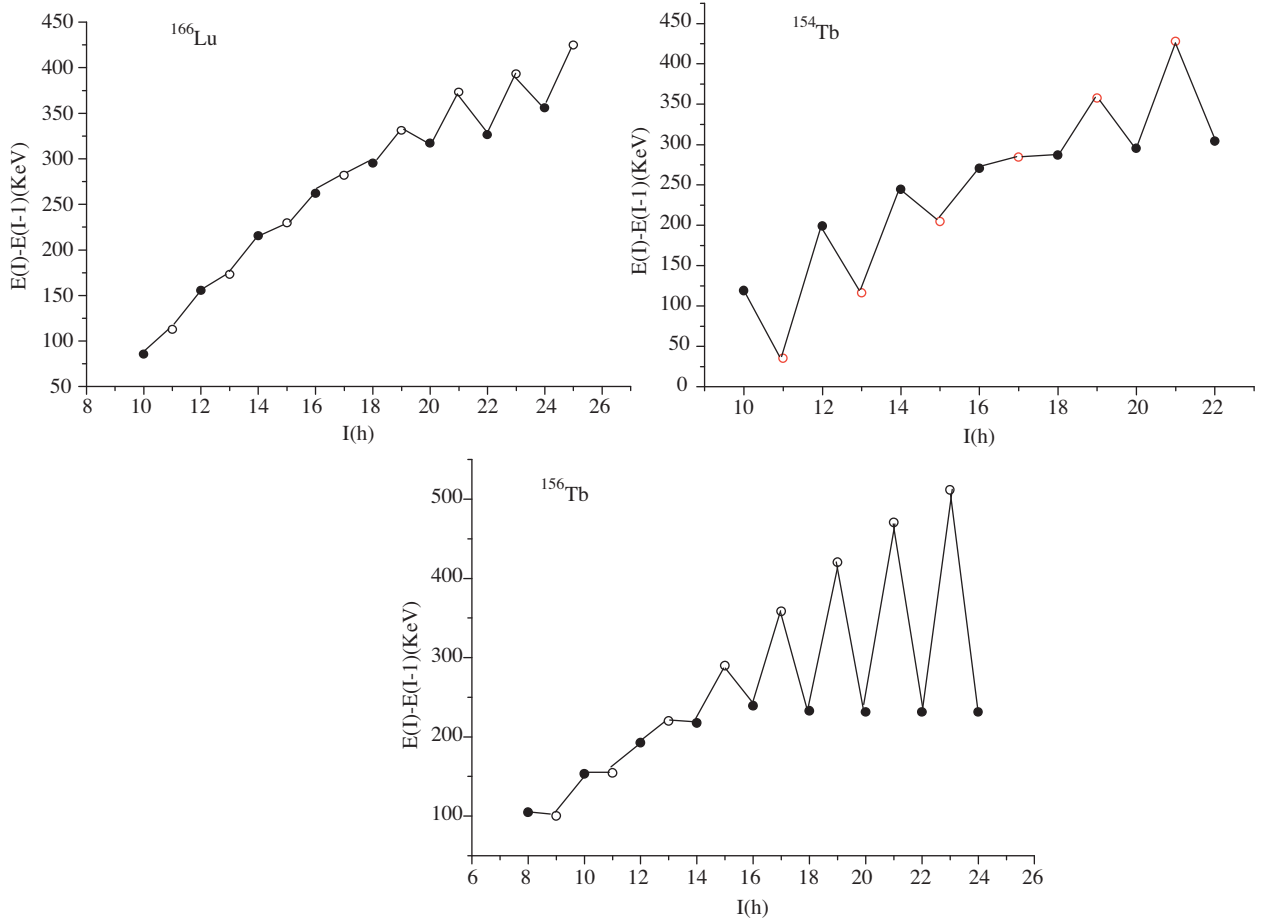


Figure 2. The same as Figure 1, but for ^{166}Lu nucleus and $^{154,156}\text{Tb}$ isotopes.

Table 1. Illustrate the calculated values of rotational frequency $\hbar\omega$ and the dynamic moment of inertia $J^{(2)}$ for ^{154}Tb .

I^π (h)	$E(I) - E(I-1)$ (KeV)	$S(I)$ (KeV)	E_γ (KeV)	$\hbar\omega$ (MeV)	$J^{(2)}$ ($\text{h}^2\text{MeV}^{-1}$)
$\alpha = 0$ (even spins)					
12^-	199.03	123.39	234.3	0.1487	31.6706
14^-	224.6	84.18	360.6	0.2089	34.904
16^-	270.5	26.0	475.2	0.2621	41.58
18^-	286.9	-34.05	571.4	0.3062	48.7804
20^-	295.2	-97.50	653.4	0.3463	50.895
22^-	304.3		732.0		
$\alpha = 1$ (odd spins)					
11^-	35.2	-123.845	154.3	0.1173	24.8756
13^-	116.14	-105.675	315.1	0.1911	29.8062
15^-	204.7	-52.85	449.3	0.2510	37.8429
17^-	284.3	5.60	555.0	0.2999	44.5434
19^-	357.6	66.55	644.8	0.3420	50.8905
21^-	427.8	128.05	723.4		

Table 2. Illustrate the calculated values of rotational frequency $\hbar\omega$ and the dynamic moment of inertia $J^{(2)}$ for ^{156}Tb .

I^π (h)	$E(I) - E(I-1)$ (KeV)	$S(I)$ (KeV)	E_γ (KeV)	$\hbar\omega$ (MeV)	$J^{(2)}$ ($\text{h}^2\text{MeV}^{-1}$)
$\alpha = 0$ (even spins)					
8^-	104.61	22.985	167.6	0.1052	46.5603
10^-	153.22	25.915	253.51	0.1501	42.7578
12^-	192.50	5.36	347.06	0.1961	44.2282
14^-	217.46	-37.35	437.5	0.2391	49.0196
16^-	229.15	-49.92	519.1	0.2775	55.6328
18^-	232.60	-156.0	591.0	0.3106	66.1157
20^-	231.30	-214.15	651.5	0.3383	79.2079
22^-	231.3	-260.0	702.0	0.3612	97.5609
24^-	231.3		743.0		
$\alpha = 1$ (odd spins)					
9^-	100.21	-28.705	204.8	0.1281	38.8915
11^-	154.4	-18.46	307.65	0.1799	38.2958
13^-	219.88	14.90	412.1	0.2297	42.1496
15^-	289.74	66.435	507.0	0.2736	49.6277
17^-	358.40	127.525	587.6	0.3101	61.0687
19^-	420.20	188.25	653.1	0.3387	81.7995
21^-	470.7	239.4	702.0	0.3612	97.5609
23^-	511.7	280.4	743.0		

Table 3. Illustrate the calculated values of rotational frequency $\hbar\omega$ and the dynamic moment of inertia $J^{(2)}$ for ^{160}Ho .

I^π (h)	$E(I) - E(I-1)$ (KeV)	$S(I)$ (KeV)	E_γ (KeV)	$\hbar\omega$ (MeV)	$J^{(2)}$ ($\text{h}^2\text{MeV}^{-1}$)
$\alpha = 0$ (even spins)					
8^-	72.99	0.665	124.09	0.0857	42.1718
10^-	115.39	1.155	218.94	0.1284	52.7217
12^-	159.89	3.24	294.81	0.1691	45.9981
14^-	203.50	1.865	381.77	0.2121	47.1142
16^-	241.83	-7.555	466.67	0.2533	50.0625
18^-	272.41	-21.135	546.57	0.2915	54.8922
20^-	296.23	-46.595	619.44	0.3261	61.0500
22^-	312.52	-79.7	684.96	0.3559	74.0192
24^-	327.0		739.0		
$\alpha = 1$ (odd spins)					
9^-	93.55	-0.64	166.54	0.1042	7.7497
11^-	134.92	-2.72	250.31	0.1470	45.6308
13^-	178.38	-3.315	337.97	0.1916	44.0868
15^-	224.89	2.225	428.70	0.2286	41.2286
17^-	273.88	16.76	525.72	0.2804	56.8828
19^-	323.21	38.89	596.04	0.3161	55.0736
21^-	372.44	68.065	668.67	0.3484	71.0101
23^-	412.0		725.0		

Table 4. Illustrate the calculated values of rotational frequency $\hbar\omega$ and the dynamic moment of inertia $J^{(2)}$ for ^{162}Tm .

I^π (h)	$E(I) - E(I-1)$ (KeV)	$S(I)$ (KeV)	E_γ (KeV)	$\hbar\omega$ (MeV)	$J^{(2)}$ ($\text{h}^2\text{MeV}^{-1}$)
$\alpha = 0$ (even spins)					
8 ⁻	48.5	1.5	74.56	0.0596	44.6927
10 ⁻	96.02	5.165	164.06	0.1086	37.5516
12 ⁻	156.79	16.28	270.58	0.1627	36.4630
14 ⁻	212.98	17.77	380.28	0.2150	40.1929
16 ⁻	256.61	6.05	479.80	0.2612	46.9153
18 ⁻	277.96	-4.495	565.06	0.3002	57.1918
20 ⁻	306.5	-22.255	635.0	0.3306	76.1904
22 ⁻	317.63	-66.71	687.5	0.3523	116.2790
24 ⁻	323.60		721.90		
$\alpha = 1$ (odd spins)					
9 ⁻	67.95	-4.31	116.45	0.0815	42.8311
11 ⁻	113.76	-12.645	209.84	0.1334	35.0140
13 ⁻	167.26	-17.625	324.08	0.1900	35.6887
15 ⁻	223.16	-11.635	436.16	0.2426	40.6545
17 ⁻	279.96	6.180	534.55	0.2875	49.3522
19 ⁻	328.57	31.845	615.60	0.3231	65.0300
21 ⁻	370.56	58.495	677.11	0.3482	103.6538
23 ⁻	398.12	77.505	715.7	—	—

Table 5. Illustrate the calculated values of rotational frequency $\hbar\omega$ and the dynamic moment of inertia $J^{(2)}$ for ^{166}Tm .

I^π (h)	$E(I) - E(I-1)$ (KeV)	$S(I)$ (KeV)	E_γ (KeV)	$\hbar\omega$ (MeV)	$J^{(2)}$ ($\text{h}^2\text{MeV}^{-1}$)
$\alpha = 0$ (even spins)					
8 ⁻	79.888	0.7935	136.445	0.0903	45.1411
10 ⁻	123.416	0.057	225.056	0.1342	46.0834
12 ⁻	166.819	0.3905	311.855	0.1767	48.0393
14 ⁻	207.295	-0.8695	395.12	0.2164	52.9941
16 ⁻	242.051	-6.4655	470.60	0.2519	59.8981
18 ⁻	269.32	-18.18	537.38	0.2840	65.1253
20 ⁻	292.3		598.80		
$\alpha = 1$ (odd spins)					
9 ⁻	101.657	0.005	181.552	0.1125	46.0156
11 ⁻	145.061	-0.0565	268.479	0.1557	46.4408
13 ⁻	187.796	0.739	354.61	0.1976	49.1642
15 ⁻	228.533	3.86	435.97	0.2366	53.6696
17 ⁻	268.500	12.8145	510.5	0.2715	61.2932
19 ⁻	306.5	25.69	575.76		

Table 6. Illustrate the calculated values of rotational frequency $\hbar\omega$ and the dynamic moment of inertia $J^{(2)}$ for ^{166}Lu .

I^π (h)	$E(I) - E(I-1)$ (KeV)	$S(I)$ (KeV)	E_γ (KeV)	$\hbar\omega$ (MeV)	$J^{(2)}$ ($\text{h}^2\text{MeV}^{-1}$)
$\alpha = 0$ (even spins)					
10 ⁻	85.5	2.25	139.5	0.1018	31.1284
12 ⁻	155.5	12.65	268.0	0.1641	33.1400
14 ⁻	215.5	14.15	388.7	0.2200	38.9483
16 ⁻	261.9	6.2	491.4	0.2671	46.6744
18 ⁻	295.2	-11.3	577.1	0.3063	56.3380
20 ⁻	317.0	-35.15	648.1	0.3369	77.8210
22 ⁻	326.3	-56.9	699.5	0.3621	80.6451
24 ⁻	355.9	-53.15	749.1		
$\alpha = 1$ (odd spins)					
11 ⁻	112.5	-8.0	198.0	0.1316	30.6044
13 ⁻	173.2	-12.3	328.7	0.1934	34.3938
15 ⁻	229.5	-9.2	445.0	0.2472	40.4858
17 ⁻	281.9	-3.35	543.8	0.2925	48.4848
19 ⁻	331.1	25.0	626.3	0.3291	62.5978
21 ⁻	373.2	51.6	690.2	0.3524	136.9863
23 ⁻	393.2	52.15	719.4	0.3750	65.1465
25 ⁻	424.9		780.8		

Table 7. Illustrate the calculated values of rotational frequency $\hbar\omega$ and the dynamic moment of inertia $J^{(2)}$ for ^{168}Lu .

I^π (h)	$E(I) - E(I-1)$ (KeV)	$S(I)$ (KeV)	E_γ (KeV)	$\hbar\omega$ (MeV)	$J^{(2)}$ ($\text{h}^2\text{MeV}^{-1}$)
$\alpha = 0$ (even spins)					
8 ⁻	63.8	-41.85	144.6	0.0906	54.4217
10 ⁻	87.6	-71.95	218.1	0.1304	46.7836
12 ⁻	115.5	-101.05	303.6	0.1743	44.4444
14 ⁻	149.1	-118.2	393.6	0.2189	45.2488
16 ⁻	321.5	80.45	482.0	0.2616	48.4848
18 ⁻	372.6	169.65	564.5	0.3003	55.4016
20 ⁻	422.8	206.25	636.7	0.3365	55.0206
22 ⁻	490.2		709.4	0.3683	73.5294
$\alpha = 1$ (odd spins)					
9 ⁻	130.5	54.8	194.3	0.1176	48.8400
11 ⁻	188.6	87.05	276.2	0.1590	47.7326
13 ⁻	244.5	112.2	360.0	0.1997	50.5689
15 ⁻	290.1	54.8	439.1	0.2381	53.7634
17 ⁻	192.0	-155.05	513.5	0.2750	54.7945
19 ⁻	213.9	-183.8	586.5	0.3071	72.0720
21 ⁻	219.2	-237.3	642.0		

Table 8. Illustrate the calculated values of rotational frequency $\hbar\omega$ and the dynamic moment of inertia $J^{(2)}$ for ^{174}Ta .

I^π (h)	$E(I) - E(I-1)$ (KeV)	$S(I)$ (KeV)	E_γ (KeV)	$\hbar\omega$ (MeV)	$J^{(2)}$ ($\text{h}^2\text{MeV}^{-1}$)
$\alpha = 0$ (even spins)					
10^-	116.3	-19.425	226.43	0.1342	47.5285
12^-	148.93	-40.255	310.59	0.1778	44.3016
14^-	182.92	-62.665	400.88	0.2222	45.771
16^-	213.53	-86.185	488.27	0.2652	47.4383
18^-	246.41	-100.5	572.59	0.3059	51.0008
20^-	282.82	-102.21	651.02	0.3435	55.4170
22^-	321.99	-90.87	723.20	0.3781	60.3045
24^-	364.8	-24.165	789.53	0.4102	64.5994
26^-	414.86	-20.61	851.45		
$\alpha = 1$ (odd spins)					
9^-	110.22	10.74	192.82	0.1176	47.1142
11^-	161.23	28.615	277.72	0.1610	44.9690
13^-	217.14	51.215	366.67	0.2060	43.9802
15^-	274.03	75.805	457.62	0.2493	48.7151
17^-	325.4	95.43	539.73	0.2888	52.6177
19^-	368.42	103.805	615.75	0.3250	58.2156
21^-	401.64	99.235	684.46	0.3576	64.9245
23^-	424.73	81.66	746.07	0.3868	72.3065
25^-	436.59	46.76	801.39	0.4126	83.6470
27^-	434.35	-11.64	849.21		

Table 9. Illustrate the calculated values of rotational frequency $\hbar\omega$ and the dynamic moment of inertia $J^{(2)}$ for ^{176}Re .

I^π (h)	$E(I) - E(I-1)$ (KeV)	$S(I)$ (KeV)	E_γ (KeV)	$\hbar\omega$ (MeV)	$J^{(2)}$ ($\text{h}^2\text{MeV}^{-1}$)
$\alpha = 0$ (even spins)					
10^-	122.4	6.7	192.9	0.1377	24.2277
12^-	197.2	5.45	358.0	0.2083	34.1296
14^-	252.6	4.15	475.2	0.2608	43.1034
16^-	294.2	0.35	568.0	0.3016	56.5770
18^-	325.5	-2.6	638.7	0.3321	78.4313
20^-	346.8	-6.35	689.7	0.3543	105.8201
22^-	364.0	-8.25	727.5	0.3738	98.7654
24^-	387.5	-3.15	768.0		
$\alpha = 1$ (odd spins)					
11^-	160.9	1.1	282.7	0.1756	29.1970
13^-	222.6	-2.3	419.7	0.2366	37.3831
15^-	274.3	0.9	526.7	0.2835	49.5049
17^-	313.4	3.55	607.5	0.3189	65.7894
19^-	342.8	6.65	668.3	0.3446	95.4653
21^-	363.5	8.1	710.2	0.3640	112.3595
23^-	381.0	5.25	745.8	0.3834	95.2380
25^-	400.3	3.5	787.8		

In ^{154}Tb the $\alpha = 1$ branch is favored up to $I = 16.5$ where a crossing of the branches take place such that the $\alpha = 0$ branch is favored at higher spins. In contrast, in the ^{168}Lu nucleus the $\alpha = 0$ branch is favored up to $I = 15.5$.

In the $^{154,156}_{65}\text{Tb}$, $^{162,166}_{69}\text{Tm}$ and $^{166,168}_{71}\text{Lu}$ isotopes, with increasing neutron number, the inversion point shifts to lower spin. The staggering magnitude of the signature dependence below the inversion point decreases with increasing neutron number. The signature inversion at the low spins is observed in the $N = 97$ and $N = 101$ isotones, it become rapidly small or it disappears in the $N = 93$ isotones, although the data are not reported in a wide range of these isotopes. For the isotones $N = 93$, the staggering magnitude below inversion point increases with increasing proton number. The change in the zigzag phase of energy difference occur at spin values at inversion points around spins $I \sim 16$, i.e. for $I \geq 16$ the favored states with even spins lie lower in energy and for $I \leq 16$ the unfavored states with odd spins lie lower in energy.

A plot of $E(I) - E(I - 1)$ as a function of I is the simplest way to identify crossing of the two signatures. The effect shows up as a reversal of the phase of the staggering. But, this effect in some odd-odd nuclei is small in magnitude; and to magnify the anomalous signature splitting, we have plotted in Figures 3 and 4 the more sensitive quantity $\delta(I)$ as a function of the spin I for our selected odd-odd nuclei with $^{154,156}\text{Tb}$, $^{162,166}\text{Tm}$, and $^{166,168}\text{Lu}$ isotopes and the (^{160}Ho , ^{162}Tm , $N = 93$), (^{166}Tm , ^{168}Lu , $N = 97$) and (^{174}Ta , ^{176}Re , $N = 101$) isotones. It is clear from these figures that the staggering magnitude of the signature dependence below the inversion point decreases with increasing N in $^{154,156}\text{Tb}$, $^{162,166}\text{Tm}$ and increases with increasing Z in the $N = 93$, $N = 97$ isotones. The inversion point shifts to lower spins with increasing N in Lu isotopes and to higher spins with increasing Z in $N = 93$ isotones. In ^{166}Lu the even-spin sequence, with the favored signature $\alpha = 0$, lies higher (yet still below) at the inversion spin $I_c = 16$ and then restores normal signature splitting with lying lower after the inversion spin. It is also noted that the inversion spin decreases with increasing neutron number. The inversion spin I_c decreases from $I_c = 16.5$ in ^{166}Lu to $I_c = 14.5$ in ^{168}Lu .

Behavior of the dynamic moment of inertia $J^{(2)}$ in doubly-odd nuclei in the $A \sim 160$ mass region is a strong indicator of their nuclear structure, particularly with regard to signature splitting of the bands. From the relative energy difference between successive $\Delta I = 2$ transition energies $E(I) - E(I - 2)$, the rotational frequency $\hbar\omega$ and the dynamic moment of inertia $J^{(2)}$ can consequently be determined. The calculated values are listed in Tables 1–9. The evolution of $J^{(2)}$ as a function of $\hbar\omega$ is illustrated in Figures 5 and 6. From these figures one notices immediately that a $\Delta I = 1$ staggering is present. It is worth noting that there are two kinds of staggering: $\Delta I = 1$ in normal deformed nuclei, as in this paper; and $\Delta I = 2$ which occurs in superdeformed nuclei [38, 39]. The spectra of some of these nuclei have also been studied [40–43] by the use of a general staggering index.

In this paper we composed the results obtained by the use of staggering indices; and to better illustrate signature inversion, one can make a plot of dynamical moment of inertia as a function of rotational frequency.

As the results shown in Figure 4 show, irregularities occur at inversion spin I_c (band crossing), above which normal behaviour is restored.

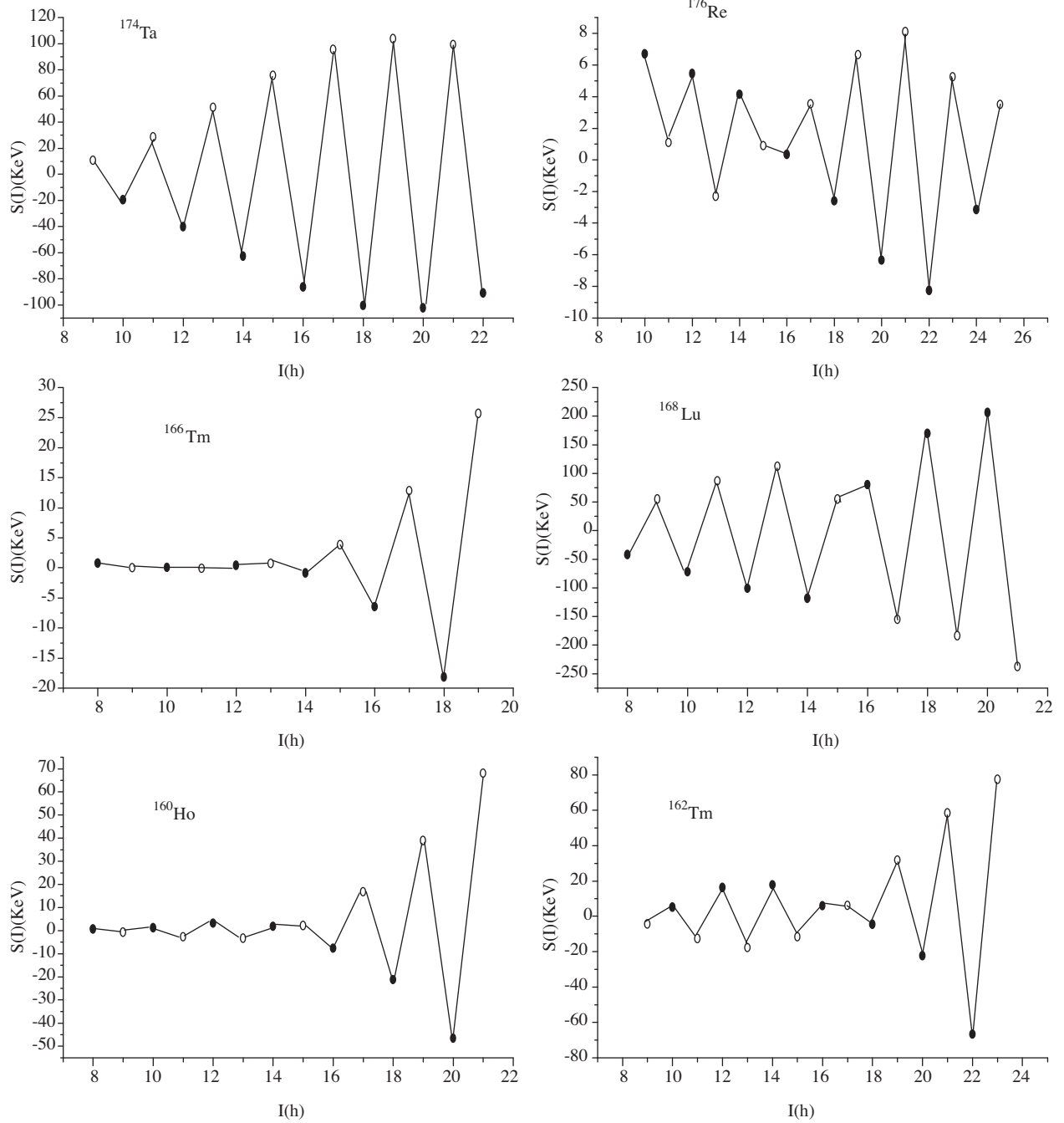


Figure 3. Systematic of signature splitting $S(I)$ defined by equation (1) versus spin I for the odd-odd isotones $N = 93$, 97 and 101. Open circles and filled circles, respectively, indicate favored signature and unfavored signature.

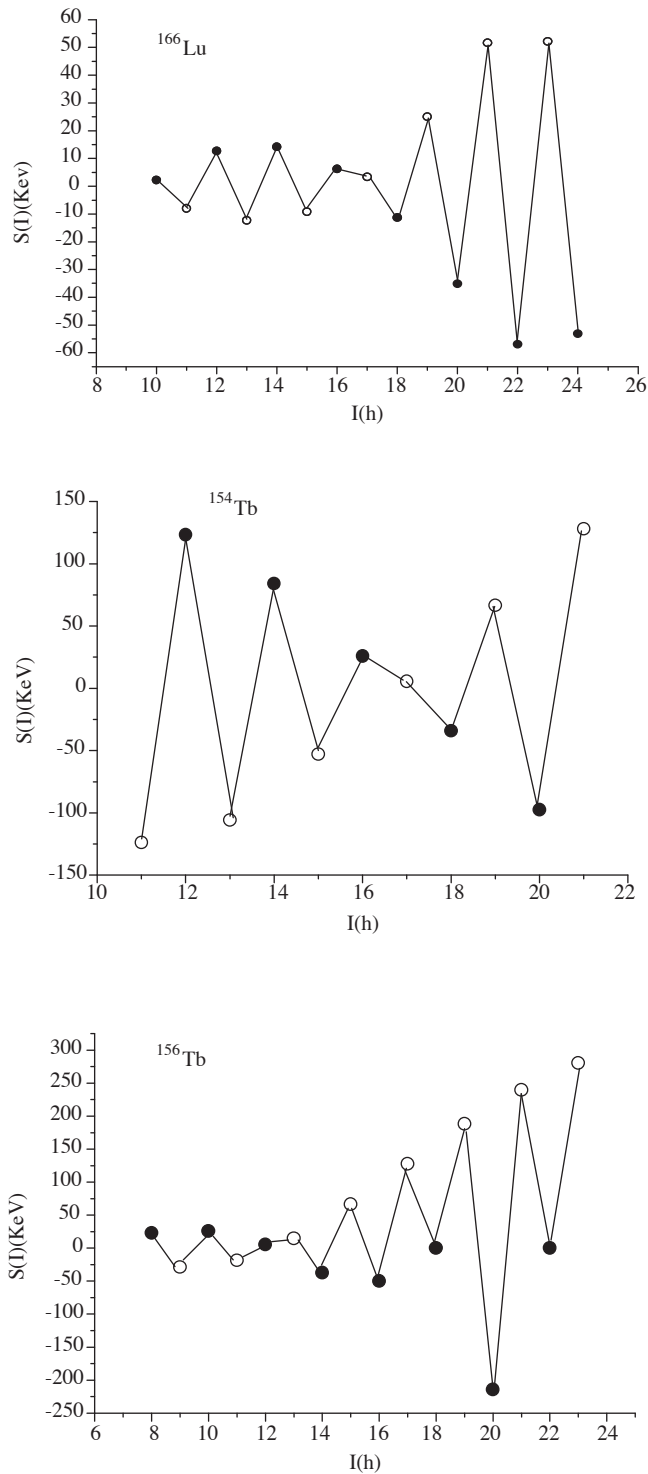


Figure 4. The same as Figure 3, but for ^{166}Lu nucleus and $^{154,156}\text{Tb}$ isotones.

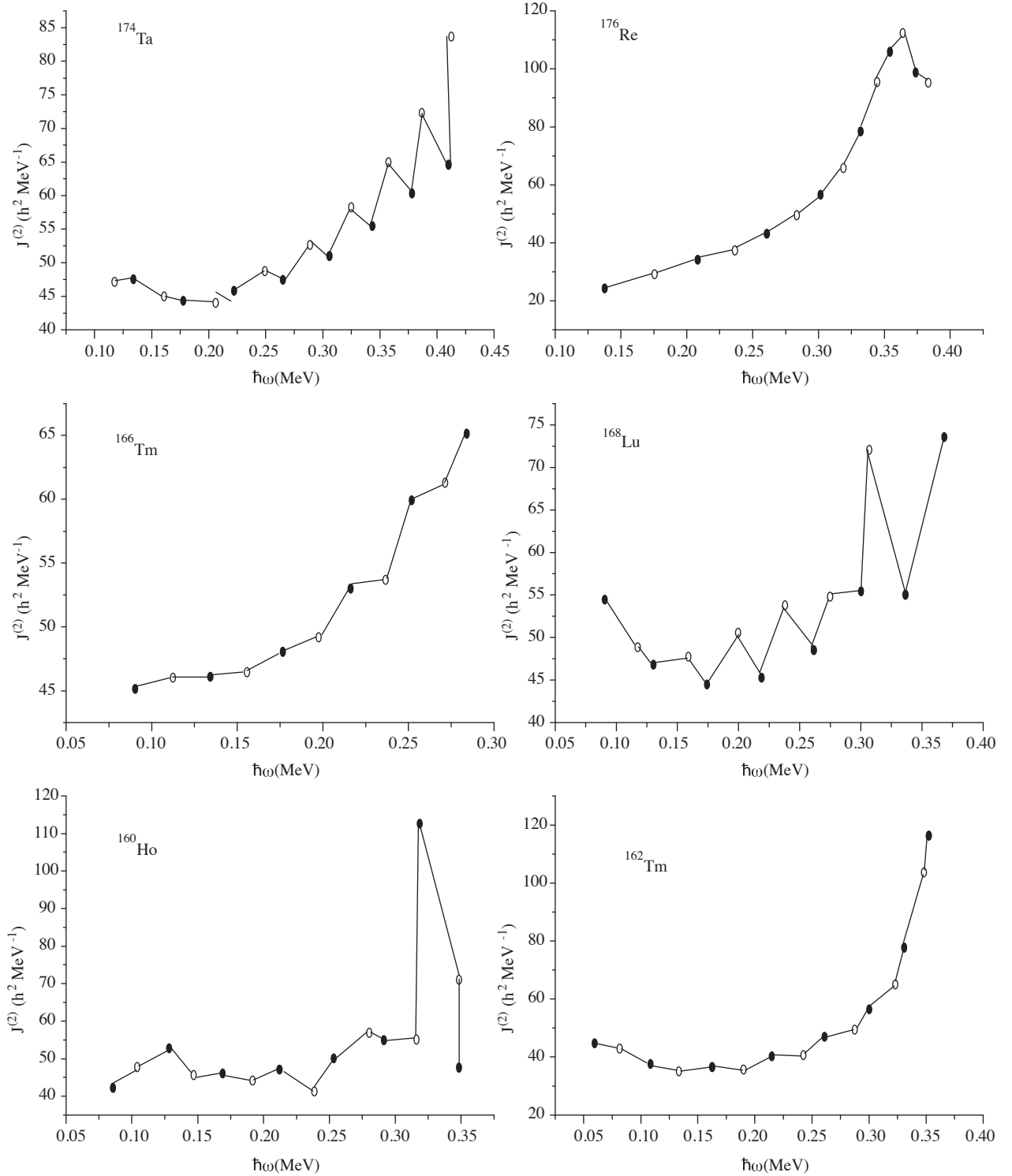


Figure 5. Plot of dynamical moment of inertia $J^{(2)}$ as a function of rotational frequency $\hbar\omega$ for the odd-odd isotones $N = 93, 97$ and 101 . The open circles and filled circles, respectively, indicate favored signature and unfavored signature.

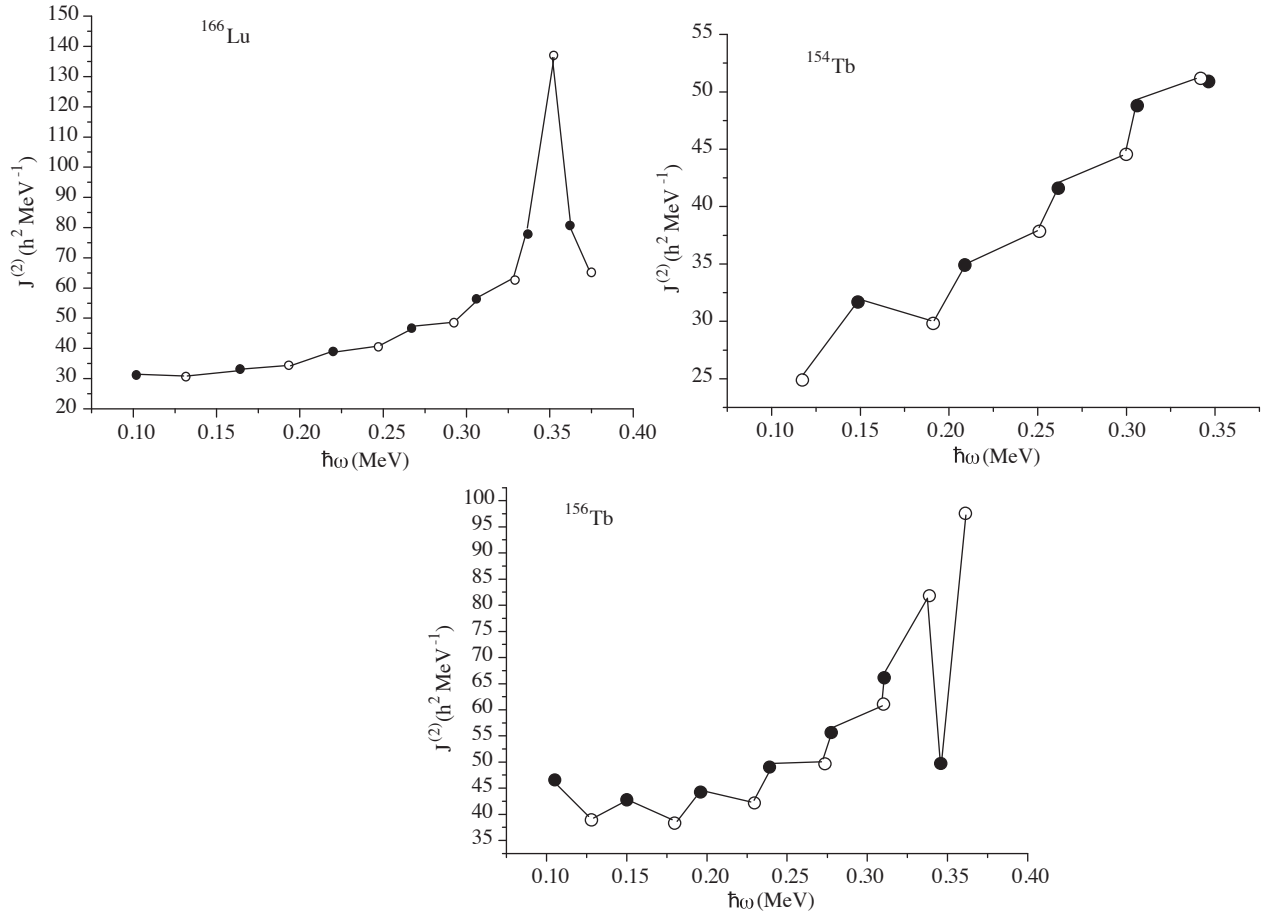


Figure 6. The same as Figure 5, but for ^{166}Lu nucleus and $^{154,156}\text{Tb}$ isotones.

References

- [1] R. W. Holf, in Proc. 8th Int. Smp. on capture gamma ray spectroscopy, Fribourg 1993, ed. J. Kern (World Scientific, Singapore 1994).
- [2] M. K. Balodis, P. T. Prokofjev, N. D. Kramer, L. I. Simonova, K. Schreckenbach, W. F. Davidson, J. A. Pinston, P. Hungerford, H. H. Schmidt, H. J. Scheerer, T. von Egidy, P. H. M. Van Assche, A. M. J. Spits, R. J. Casten, W. R. Kane, D. D. Warner and J. Kern., *Nucl. Phys.*, **A472**, (1987), 445.
- [3] D. Hojman , M. A. Cardona, M. Davidson, M. E. Debray, A. J. Kreiner, F. Le Blanc, A. Burlon, J. Davidson, G. Levinton, H. Somacal, J. M. Kesque, F. Naab, M. Ozafran, P. Stolar, M. Vazquez, D. R. Napoli, D. Bazzacco, N. Blasi, S. M. Lenzi, G. Lo Bianco and C. Rossi Alvarez, *Phys. Rev.*, **C61**, (2000), 064322.
- [4] D. Hojman, A. J. Kreiner, M. Davidson, J. Davidson, M. Debray, E. W. Cybulski, P. Pascholati and W. A. Seale, *Phys. Rev.*, **C45**, (1992), 90.
- [5] J. H. Ha, J. C. Kim, C. S. Lee, J. H. Lee, J. Y. Huh, C. B. Moon, S. J. Chae, K. Furuno, T. Komatsutara, T. Schizuma, K. Matsuura, K. Kato, Y. Sadaki, H. Ishiyama, Y. Gono, T. Morikawa, S. Mitarai, M. Shibata, H.

- Watababe, M. Miyake, E. Komatsu, A. Odahara, E. Ldeguchi, and X. H. Zhou, *Journal of Physical Society of Japan*, **71**, (2002), 1663.
- [6] M. A. Cardona, A. J. Kreiner, D. Hojman, G. Levinton, M. E. Debray, M. Davidson, J. Davidson, R. Pirchio, H. Somacal, D. R. Napoli, D. Bazzacco, N. Blasi, R. Burch, D. De Acuna, S. M. Lenz G. Lo Bianco, J. Rico, and C. Rossi Alvarez, *Phys.Rev.*, **C59**, (1999), 1298.
- [7] M. A. Cardona, J. Davidson, D. Hojman, M. E. Debray, A. J. Kreiner, H. Somacal, M. Davidson, D. R. Napoli, D. Bazzacco, N. Blasi, R. Burch, D. De Acuna, S. M. Lenzi, G. Lo Bianco, J. Rico, and C. Rossi Alvarez, *Phys. Rev.*, **C56**, (1997), 707.
- [8] R. A. Bark, H. Carlsson, S. J. Freeman, G. B. Hagemann, F. Ingebretsen, H. J. Jensen, T. Lönnroth, M. J. Piiparinens, I. Ragnarsson, H. Ryde, H. Schnack-Petersen, P. B. Semmes and P. O. Tjøm, *Nucl. Phys.*, **A630**, (1998), 603.
- [9] R. A. Bark, J. M. Espino, W. Reviol, P. B. Semmes, H. Carlsson, I. G. Bearden, G. B. Hagemann, H. J. Jensen, I. Ragnarsson, L. L. Riedinger, H. Ryde, and P. O. Tjøm, *Phys.Lett.*, **B406**, (1997), 193.
- [10] S. Drissi, Ziping Li, M. Délèze, J. Kern, J. P. Vorlet, *Nucl. Phys.*, **A600**, (1995), 63.
- [11] S. Drissi, S. André, D. Barnéoud, C. Foin, J. Genevey and J. Kern, *Nucl. Phys.*, **A601**, (1996), 234.
- [12] S. L. Gupta, S. C. Pancholi, P. Juneja, D. Mehta, Ashok Kumar, R. K. Bhowmik, S. Muralithar, G. Rodrigues, and R. P. Singh, *Phys.Rev.*, **C56**, (1997), 1281.
- [13] S. K. Katoch, S. K. Katoch, S. L. Gupta, S. C. Pancholi, D. Mehta, S. Malik, G. Shanker, L. Chaturverdi and R. K. Bhowmik, *Z. Phys.*, **A358**, (1997), 5.
- [14] S. J. Mannanal, B. Boschung, M. W. Carlen, J. Cl. Dousse, S. Drissi, P. E. Garreett, J. Kern, B. Perny, Ch. Rheme, J. P. Vorlet, C. Gunthe, J. Manns and U. Muller, *Nucl. Phys.*, **A582**, (1995), 141.
- [15] Y. H. Zhong, X. H. Zhou, Q. Zhao, X. F. Sun, X. G. Lei, Y. X. Guo, Z. Liu, X. F. Chen, Y. T. Zhu, S. X. Wen, G. J. Yuan and X. A. Liv, *J. Phys.*, **G23**, (1997), 723
- [16] Y. H. Zhong, X. H. Zhou, Q. Zhao, X. F. Sun, X. G. Lei, Y. X. Guo, Z. Liu, X. F. Chen, Y. T. Zhu, S. X. Wen, G. J. Yuan and X. A. Liv, *Z. Phys.*, **A355**, (1996), 335.
- [17] A. J. Kriener, *Phys. Rev.*, **C38**, (1988), R2486.
- [18] J. Y. Zeng, S. X. Liu, Y. A. Lie, L. Yu, *Phys. Rev.*, **C63**, (2001), 024305.
- [19] L. B. Karlsson, I. Ragnesson and S. Aberg, *Phys. Lett.*, **B416**, (1998), 16.
- [20] R. F. Costen, N. V. Zamfir, P. Von Brentano and W. T. Chou, *Phys. Rev.*, **C45**, (1992), R1413.
- [21] K. Haro and Y. Sun, *Nucl. Phys.*, **A529**, (1991), 445.
- [22] W. Reviol, H. Q. Jin and L. L. Riedinger, *Phys.Lett.*, **B371**, (1996), 19.
- [23] R. Bengtsson, H. Frisk and F. R. May, *Nucl. Phys.*, **A415**, (1984), 89.

- [24] R. Bengtsson, J. A. Pinston, D. Barneoud, E. Monnand and F. Schussler, *Nucl. Phys.*, **A389**, (1982), 158.
- [25] D. Barneaud et al, *Z.Phys.*, **A314**, (1983), 69.
- [26] J. A. Pinston et al, *Phys.Lett.*, **137B**, (1984), 47.
- [27] G. Lovhoiden, *Phys.Scipta*, **25**, (1982), 459.
- [28] K. Hara and Y. Sun, *Nucl. Phys.*, **A531**, (1991), 221.
- [29] K. Hara, *Nucl. Phys.*, **A557**, (1993), 449c.
- [30] R. Bengtsson, *Nucl. Phys.*, **A437**, (1985), 263.
- [31] I. Hamamoto, *Phys.Lett.*, **B235**, (1990), 221.
- [32] P. Semmes and I. Ragnsson, *International Conference on High-Spin Physics And Gamma Soft Nuclei*, Pittsburgh, 1990 (World Scientific, Singapore 1991)
- [33] R. R. Zherg, S. Q. Zhu and Y. W. Pu, *Phys.Rev.*, **C56**, (1997), 175.
- [34] A. K. Jain, J. Kvasil, R. K. Sheline and R. W. Hoff, *Phys.Rev.*, **C40**, (1989), 432.
- [35] A. K. Jain and A. Goel, *Phys.Lett.*, **B277**, (1992), 233.
- [36] N. Yoshida, H. Sagawa and J. Otsuka, *Nucl. Phys.*, **A567**, (1994), 17.
- [37] B. Singh, *Nuclear Data Sheets*, **107**, (2006).
- [38] A. M. Khalaf and M. M. Sirag, *Egypt.J.Phys.*, **35**, (2004), 359.
- [39] M. M. Sirag, *Egypt.J.Phys.*, **38**, (2007), 1.
- [40] Y. Lin, Y. Ma, H. Yang and S. Zhou, *Phys. Rev.*, **C52**, (1995), 2514.
- [41] G. Garcia Bermudez and M. A. Cardona, *Phys. Rev.*, **C64**, (2001), 034311.
- [42] M. A. Cardon, D. Hojman, M. E. Debray, A. K. Kreiner, M. Davidson, J. Davidson, D. R. Napoli, D. Bazzacco, N. Blasi, S. M. Lenzi, G. Lo Bianco and C. Rossi Alvarez, *Phys. Rev.*, **C66**, (2002), 044308.
- [43] R. Zheng, R. Zheng, S. Zhu, N. Cheng and J. Wen, *Phys. Rev.*, **C64**, (2001), 014313.